Experimental Study of Interacting Vortex Rings

By

Naoki IZUTSU, Koichi OSHIMA and Yuko OSHIMA*

(February 5, 1987)

Summary: Interactions of vortex rings were experimentally studied by means of hot wire anemometers. Velocity fields were measured in single, two coaxial and two parallel axial vortex rings. The vorticity fields calculated from the obtained data were animated and were quantitatively analyzed in order to explain the interacting mechanism. The results clearly demonstrate the processes of the merging, splitting, crosslinking and decay of the vortical regions..

1. INTRODUCTION

A motion of vortex ring is one of the basic and familiar phenomena of vortical flow and is easily realized both in nature and in the laboratory through visualization. One of the authors had carried out a series of experiments for the interaction of vortex rings by flow visualization. The vortices which are placed in an unbounded space can interact and change their form with time. Merging, splitting and crosslinking may occur depending on the initial conditions. So far most experimental researches have been done with the help of flow visualization by such as smoke, dye, Schlieren methods nevertheless these methods show the sum of fluid streaks and do not always prove existence of vorticity or cannot visualize a vortex ring itself. In particular, interaction of vortex rings causes severe aberration between streak lines and vorticity distributions. Since a vortex in a rotational motion is expressed by nonzero vorticity, no streak method but measurement of vorticity is suitable for the study of interacting vortical regions. Due to the direct measurement of vorticity is rather difficult, computation of vorticity from measured velocity field is substituted.

In this paper interaction of vortex rings was experimentally studied by means of hot wire anemometers in three basic configurations of vortex rings as shown in Fig. 1. The first case is one vortex ring (single case), the second one is two vortex rings moving along the common axis (two coaxial case), and the last case is two vortex rings proceeding side by side along their parallel axes (two parallel case). Their interacting, merging and crosslinking processes were investigated through computer aided experiments.

A circular vortex ring is created by ejection of air through a circular orifice for an instant, and it moves perpendicularly to its plane. In order to get the velocity field, phase locked time records of velocity are obtained point by point at every position

* Faculty of Science, Ochanomizu University

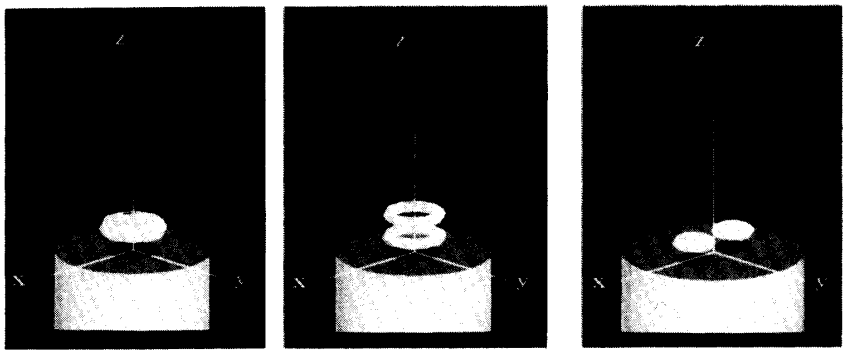

Fig. 1. Vortex configuration and coordinate system, (a) Single vortex ring, (b) Two coaxial vortex rings, (c) Two parallel axial vortex rings.

throughout the measurement volume. Reproducibility of this phenomenon is actually required so as to sort these data for time in the whole field.

The origin of coordinates is set at the center of the circular orifice with the diameter of D. It is considered the phenomena of one hole cases are axisymmetric. In two holes case, the origin is set at the middle point between their centers with a distance L. The z axis is taken perpendicularly to the orifice and the x and y axes are at right angles to it. Here, u, v and w denote the velocity components in the directions of x, y and z, respectively. The Reynolds number of experiments is defined as

$$Re = DV/2\nu, \tag{1}$$

where V is the maximum mean velocity at the outlet of the orifice and ν is the kinematic viscosity of the fluid.

2. Method

Figure 2 shows the general schematic of data processing system composed of three stages. The first stage is the experimental measurements whose parameters are determined by the orifice, the vortex configuration and the Reynolds number of the experiments, which is controlled by the ejection velocity changing pressure of the air reservoir. The opening duration of the electric valve ΔT determines the number of vortex rings along the same axis. The second stage is getting of the velocity field at every instant through sorting from sequentially stored velocity record with time at every position, and then vorticity fields at every instant are computed. Before sorting, the velocity data are operated with a low pass filter so that every datum could smoothly connected with all of neighboring data. The last stage is analyzing the physical quantities such as peak vorticity, circulation, traveling distance, traveling velocity, effective radius, core radius, fluid impulse, enstrophy of the vorticity field.

The measurement schematic is presented in Fig. 3. Vortex rings are generated by ejection of air through a circular orifice. The number of vortex rings along the same axis is determined by the opening duration of the electric valve which is controlled by

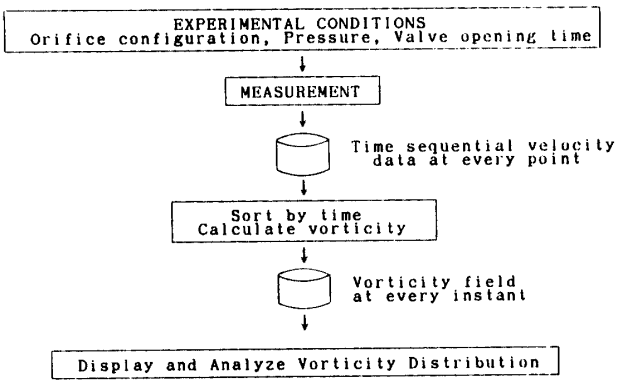

Fig. 2. Data processing system.

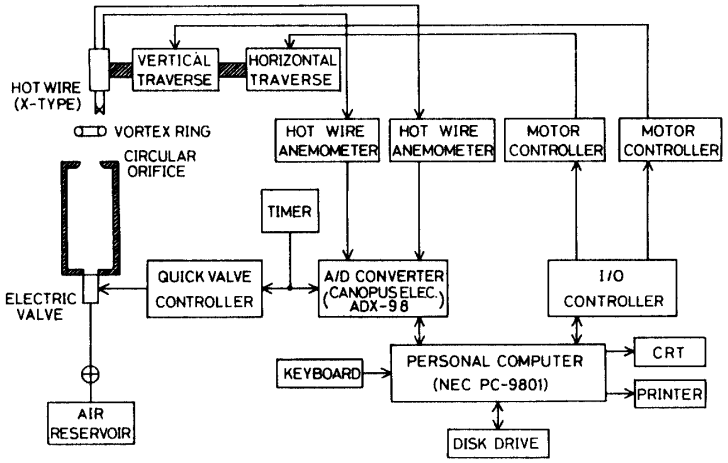

Fig. 3. Schematic of the measurement.

the quick valve controller. The X type hot wire is traversed with the intervals of Δx, Δy and Δz in the measurement area or volume over the orifice. The velocities were measured at every Δt time interval during t_{max} time. The flow chart of the measurements is expressed in Fig. 4. Four times of data are ensemble averaged at every position owing to the fairly good reproducibility. All measurement equipments are controlled by the laboratory personal computer. The time base of the measurement system are set by a pulse of timer which make a pulse at every 1.5 seconds. The images of vorticity fields are animated and the variations of the quantitative values are displayed as the functions of time.

On the other hand, Schlieren method is adopted to visualize of the flow field as a function of time using time delay and strobo flashing. Experimental conditions are summarized in Tables 1 and 2.

3. Results

Figures 5 (a)-(c) are series of the photographs taken by Schlieren method corresponding to three cases, respectively. In the two coaxial case, passing through motion is observed before merging into one as shown in (b). As a repetition of passing through motion depends on the Reynolds number or the initial velocity of the ring,

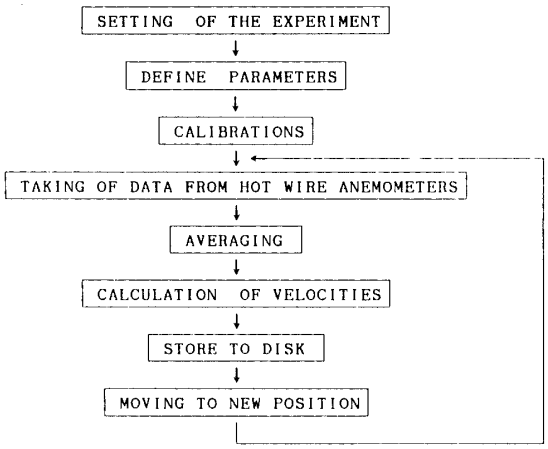

Fig. 4. Flow chart of the measurement.

Table 1. Orifices used in the experiments

Orifice	The number of holes	D mm	L mm
A	1	20	—
B	2	13	21

Table 2. Experimental conditions

Case	Orifice	P kg/cm^2	ΔT ms	Δt ms	t_{max} ms	Δx mm	Δy mm	Δz mm	x mm	y mm	z mm
1	A	0.3	2	0.2	38.2	1	—	1	−2~24	0	2~80
2	A	0.35	2	0.2	38.2	1	—	1	−2~24	0	2~80
3	A	0.35	2	0.4	76.4	2	—	2	−2~24	0	2~256
4	A	0.3	5	0.2	38.2	1	—	1	−2~30	0	2~80
5	A	0.35	5	0.2	38.2	1	—	1	−2~30	0	2~80
6	A	0.35	5	0.4	76.4	2	—	2	−2~30	0	2~256
7	B	0.3	2	0.2	38.2	1	—	1	−2~36	0	2~80
						—	1	1	0	−2~36	2~80
8	B	0.35	2	0.2	38.2	1	—	1	−2~36	0	2~80
						—	1	1	0	−2~36	2~80
9	B	0.3	2	0.2	38.2	1.6	1.6	1.6	0~25.6	0~25.6	2~74

one can realize the repetition of the passing through game before the rings merging at higher pressure of the reservoir. In the two parallel axial case, two side views perpendicularly to each other are presented in the upper and the lower pictures in (c), respectively. Two vortex rings approach each other and merge into one after being switched, and it may split again into two rings in the plane perpendicularly to the original one under a certain condition.

Figures 6 (a) and (b) show the time development of the velocity distribution near the outlet and the maximum and mean value of the velocity for single ring of Case 2. From Fig. 6 (a), we can clearly image the generation of a vortex ring.

The color coded vorticity distributions on the cross section are displayed in Figs. 7

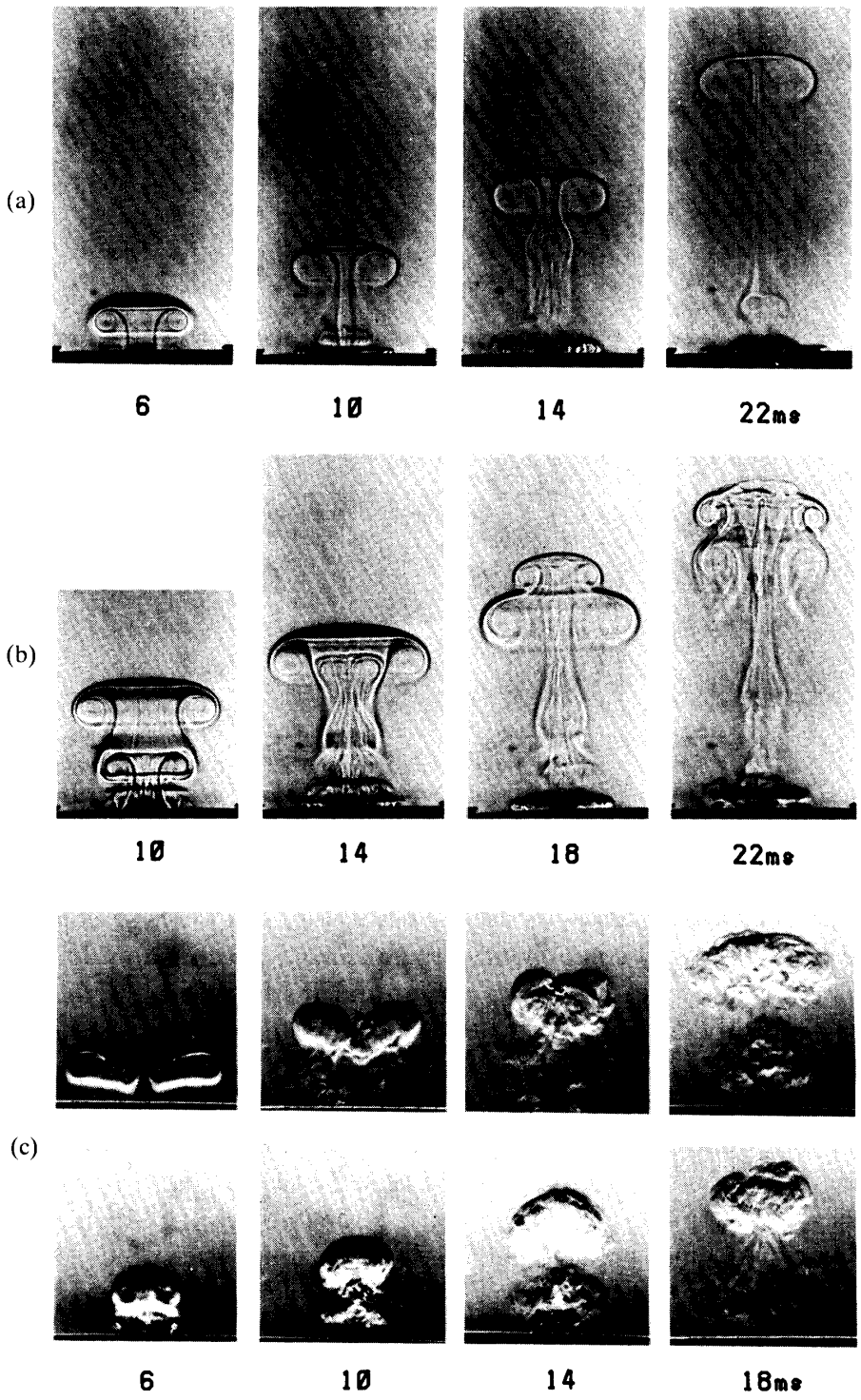

Fig. 5. Photographs taken by Schlieren method, (a) Case 2, (b) Case 5 and (c) Case 7, upper and lower pictures show two side views perpendicularly to each other.

(a)-(c), in which the vorticity values are transformed into one of the color codes of blue to red. Green corresponds to null vorticity. They clearly demonstrate the interacting processes of vortical regions. In the two parallel case, two cross sectional

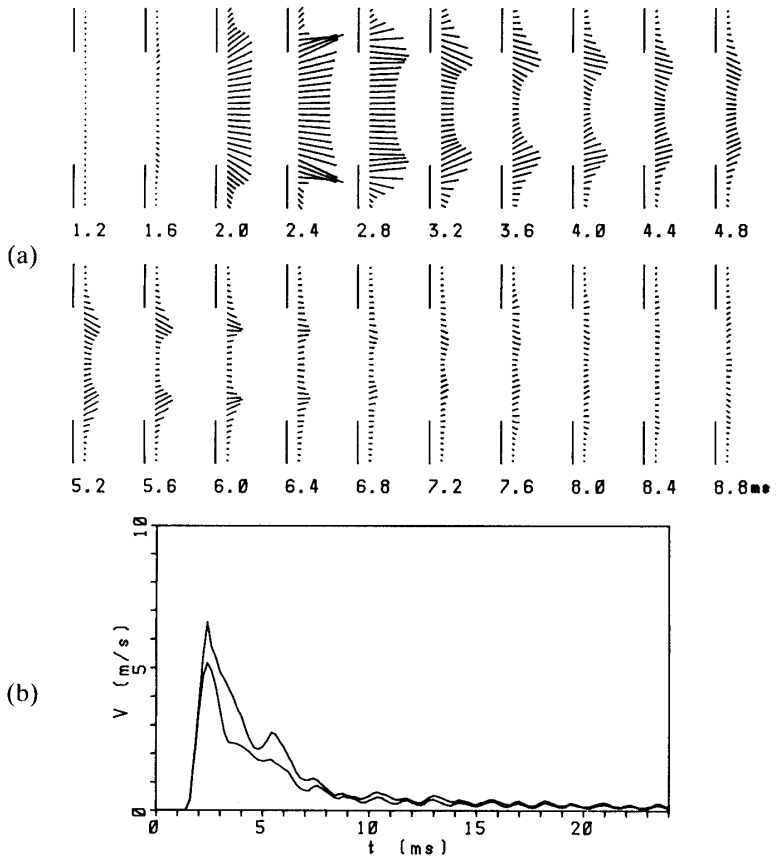

Fig. 6. Velocity distribution near the outlet (a) and the maximum and mean value of velocity (b) in Case 2.

views, the x-z and y-z plane views are shown in Fig. 7 (c). Those colors show the magnitude of the vorticity component perpendicular to each plane. It is found that two rings merge into one in the x-z plane, and in the side view the crosslinked vorticity currents produce between two rings in the y-z pane. It is more clearly proved through the perspective views in Figs. 8 (a)-(d). (a) and (b) are two side views perpendicularly each other, (c) is the front view and (d) is perspective view. In these figures, the magnitude of the absolute vorticity is perspectively presented. If we have eyes to see the vorticity directly, one can observe as the sight of these pictures.

From these results, the process of the crosslinking mechanism is explained as follows. Two vortex rings proceed and approach to touch each other. Then parts of them are gradually crosslinked (t=6ms), and their bypass currents are forced to be pushed down and stretched to the sides by induced velocity. At this stage, parts of the precede two rings still remain, and a saddle shape vortex is formed (t=12ms). Finally the new ring breaks away from the first ones which rapidly decay. Thus two rings become one. Consequently an elliptic vortex ring is left in the flow field, and it proceed forward oscillately.

This mechanism is verified quantitatively by Fig. 9. The circulation of first rings Γ_x, the crosslinked bypass current or new ring grown behind the previous rings Γ_{xy} and the secondary ones on the other way Γ_y are plotted as the function of time. It shows that parts of the circulations of precede two rings are converted into the crosslinking

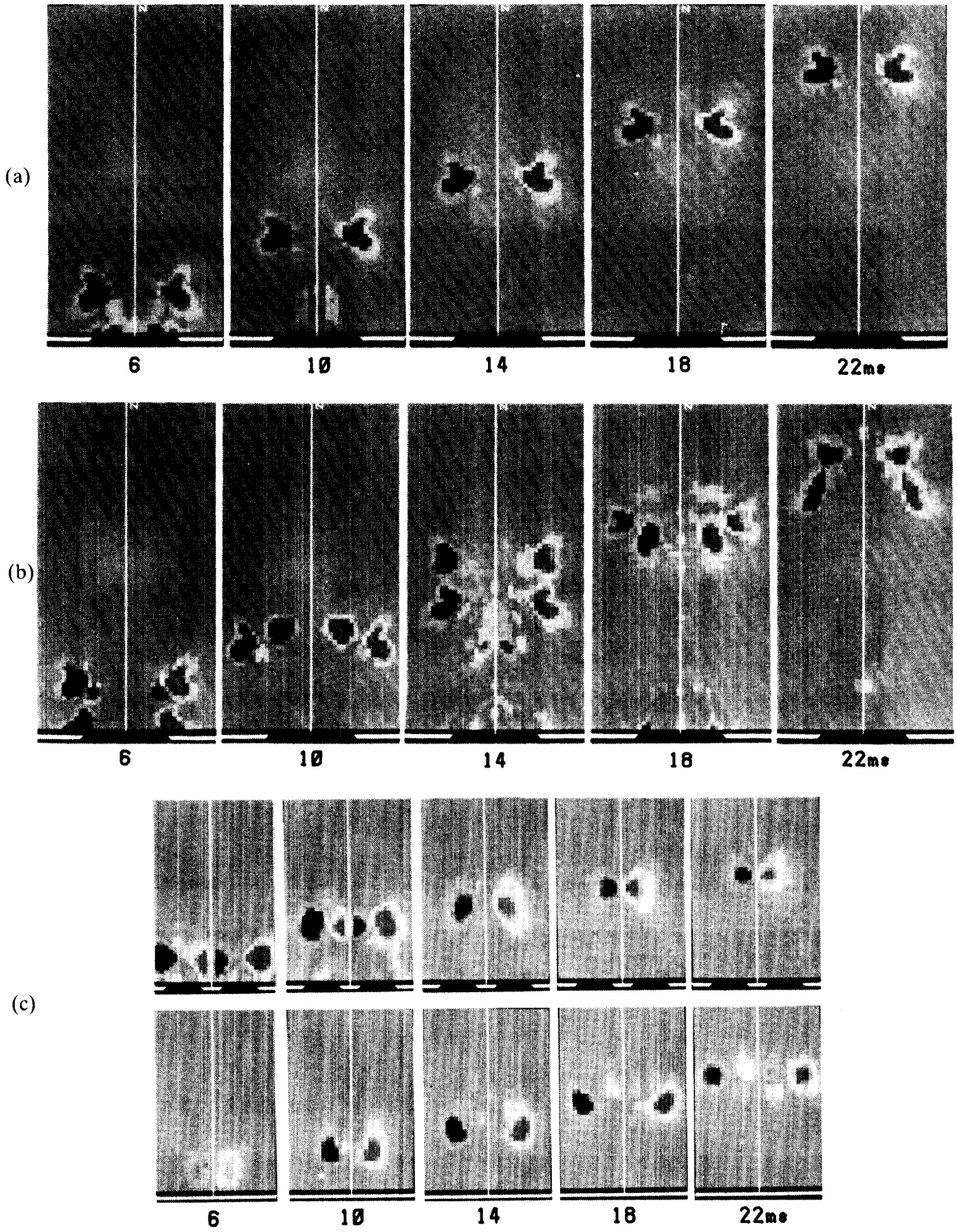

Fig. 7. Cross sectional views of color coded vorticity distribution, (a) Case 2, (b) Case 5, (c) Case 9.

and the rest of them will decay. On the other hand, a new ring behind them are created by crosslinking and it seems to grow by itself. However, it is not well known whether the energy of growth is coming from the precede rings or not. Concerning this point it is necessary to do more precise experiments.

On the other hand, quantitative analyze in the single and coaxial cases was carried

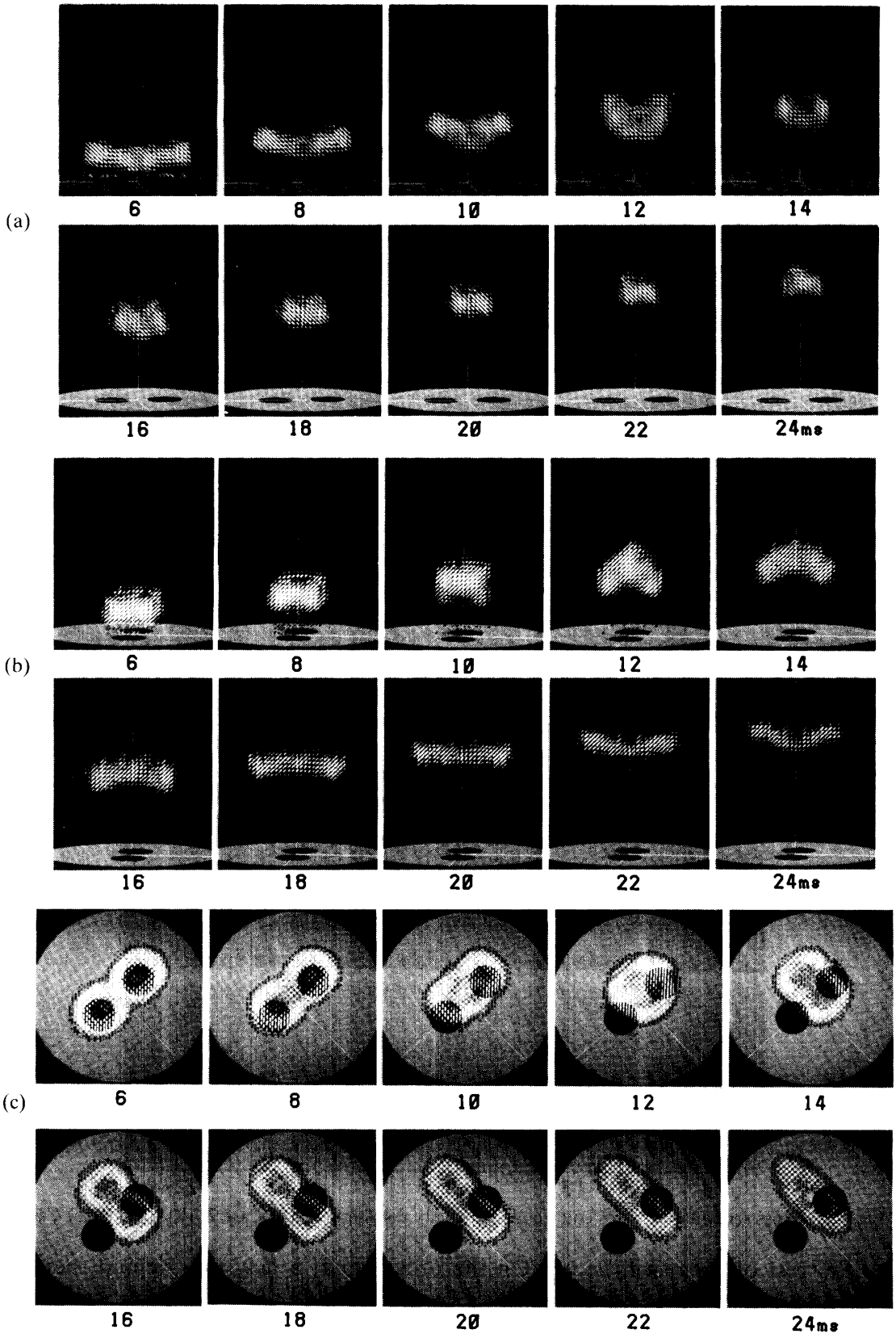

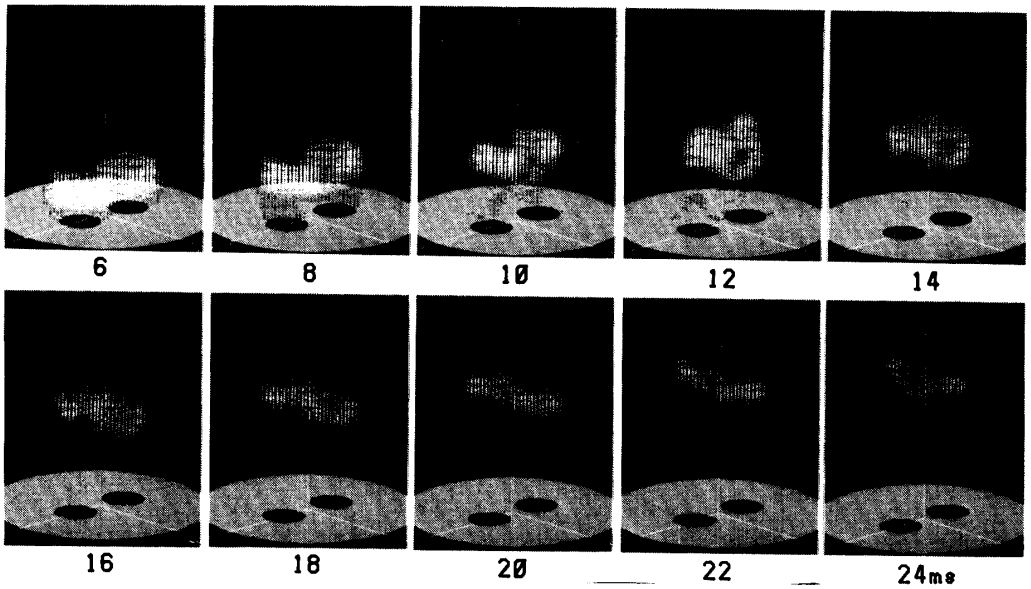

Fig. 8. Time development of two vortex rings side by side in Case 9, (a), (b) Two side views, (c) Front view, (d) Perspective view.

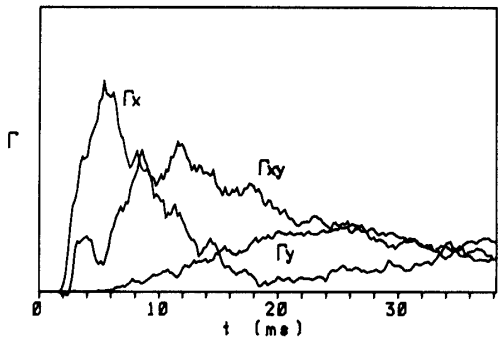

Fig. 9. Development of the circulation in Case 9.

out and the results are shown in Figs. 10 (a)-(h). The time t, peak vorticity ω_{max}, circulation Γ, traveling distance z and speed, U, effective radius R, core radius σ, fluid impulse P, enstrophy E are nondimensionalized by the initial circulation Γ_0' and the diameter of the orifice D. The value at $t'=7$ms is selected as the initial state. where the prime indicates dimensional values and $r=\sqrt{x^2+y^2}$.

In the two coaxial case, the peak value of vorticity is decreased when passing through motion occur. It is considered as the concentration of the vorticity of the precede vortex ring is decreased because of reduction of core radius and increase of effective radius. The peak vorticity and circulation decrease as the time increase. The traveling speed is suddenly decrease after merging, as shown in Fig. 10 (c) and (d). It is considered that the merging promote to mix and decay the rings. The effective radius of the vortex ring decreases with increasing time in single case but it is rather increase just after merging in two coaxial case as shown in Fig. 10 (e). The core radii keep almost constant as shown in Fig. 10 (f). Fluid impulse and enstrophy are reduced rapidly just after merging as shown in Figs. 10 (g) and (h).

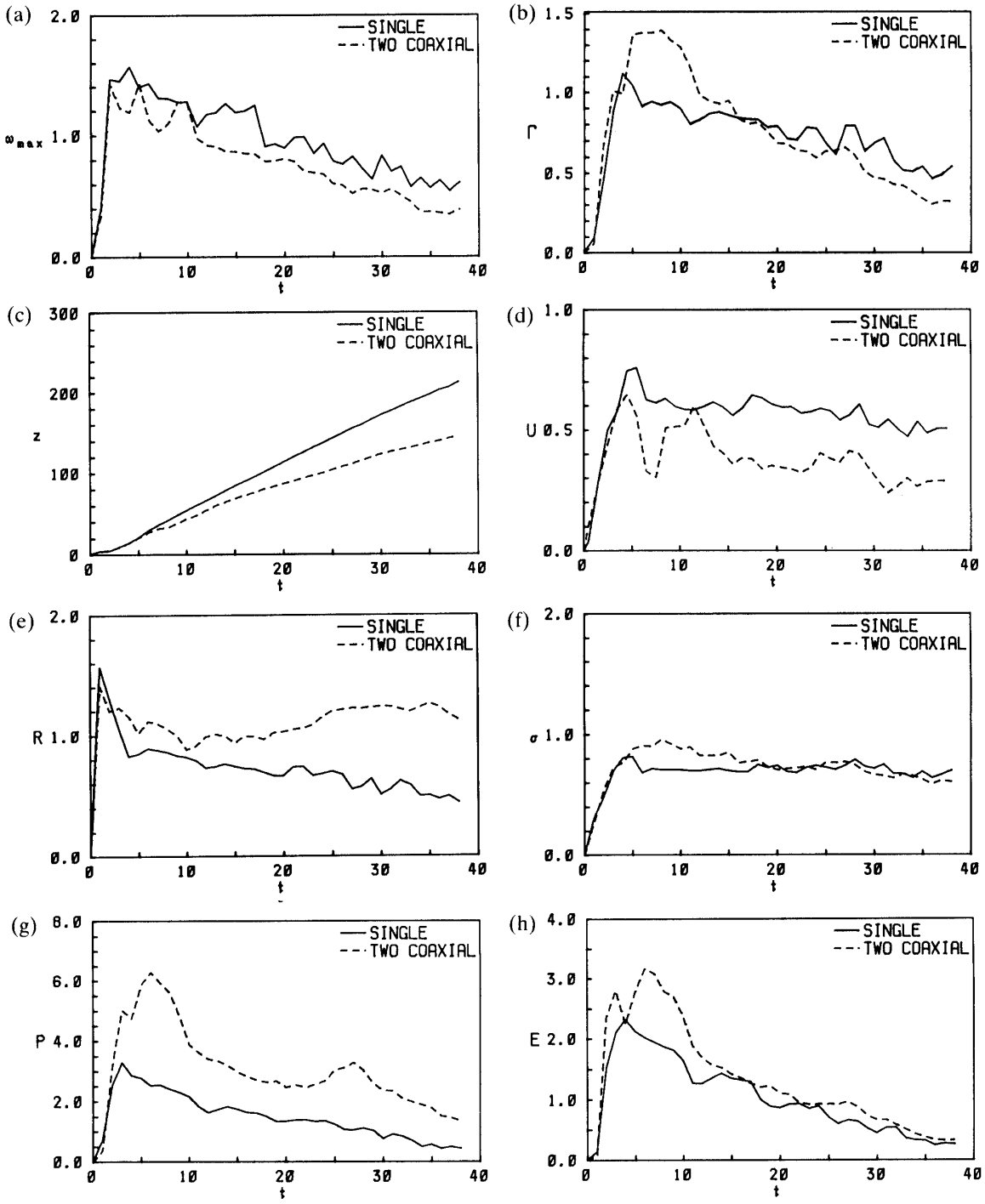

Fig. 10. Variation of the quantitative values with time in Case 2 and 5.

(a) Peak vorticity	(e) Effective radius
(b) Circulation	(f) Core radius
(c) Traveling distance	(g) Fluid impulse
(d) Traveling speed	(h) Enstrophy

$$t = 4t'\Gamma'_0/D^2, \tag{2}$$

$$\omega_{\max} = \omega'_{\max} D^2/4\Gamma'_0, \tag{3}$$

$$\Gamma = \Gamma'/\Gamma'_0, \tag{4}$$

$$z = 2z'/D, \tag{5}$$

$$U = U'D/2\Gamma'_0, \tag{6}$$

$$R = 2R'/D, \tag{7}$$

$$\sigma = 2\sigma'/D, \tag{8}$$

$$P = \pi \iint 4r^2\omega' dr dz/\Gamma'_0 D^2, \tag{9}$$

$$E = \pi \iint rD\omega'^2 dr dz/2\Gamma'^2_0, \tag{10}$$

4. Conclusions

The velocity field around interacting vortex rings was measured by hot wire anemometers. The vorticity fields was calculated and animated which clearly demonstrates merging and splitting processes of vortical regions.

A new crosslinking process was found in the interacting process of two vortex rings proceeding side by side along their parallel axes. That is, parts of the circulations along their rings are crosslinked after being switched. The new concentration of vorticity grows to make a vortex ring and the rest of them is rapidly vanished and an oscillating elliptic vortex ring is left.

References

[*1*] Kambe, T. and Oshima, Y.: Generation and decay of viscous vortex flow, J. Phys. Soc. Japan, **38** (1975) 271–280.

[*2*] Oshima, Y., Kambe T. and Asaka, S.: Interaction of two vortex rings moving along a common axis of symmetry, J. Phys. Soc. Japan, **38** (1975) 1159–1166.

[*3*] Oshima, Y. and Asaka, S.: Interaction of two vortex rings along parallel axes in air, J. Phys. Soc. Japan, **42** (1977) 708–713.

[*4*] Oshima, Y. and Asaka, S.: Interaction of multi-vortex rings, J. Phys. Soc. Japan, **42** (1977) 1391–1395.

[*5*] Oshima, Y.: Head-on collision of two vortex rings, J. Phys. Soc. Japan, **44** (1978) 328–331.